2014

Compressor with Turning-Paired Vane and Piston

Kiyoshi Sawai
Hiroshima Institute of Thechnology, sawai@me.it-hiroshima.ac.jp

Manabu Doi
Hiroshima Institute of Thechnology, a310083@cc.it-hiroshima.ac.jp

Noriaki Ishii
Osaka Electro Communication University, ishii@isc.osakac.ac.jp

Hiroaki Nakai
Panasonic Corporation, nakai.hiroaki@jp.panasonic.com

Hirofumi Yoshida
Panasonic Corporation, yoshida.hirofumi@jp.panasonic.com

See next page for additional authors

Authors
Kiyoshi Sawai, Manabu Doi, Noriaki Ishii, Hiroaki Nakai, Hirofumi Yoshida, and Takashi Morimoto

Compressor with Turning-paired Vane and Piston

Kiyoshi SAWAI[1]*, Manabu DOI[1], Noriaki ISHII[2]
Hiroaki NAKAI[3], Hirofumi YOSHIDA[3], Takashi MORIMOTO[3]

[1]Hiroshima Institute of Technology, Dept. of Mechanical Engineering
Hiroshima, Japan
Phone: +81-82-921-5475, E-Mail: sawai@me.it-hiroshima.ac.jp

[2]Osaka Electro Communication University, Dept. of Mechanical Engineering
Osaka, Japan
Tel/fax: +81-72-820-4561, E-mail: shii@isc.osakac.ac.jp

[3]Panasonic Corporation, Appliances Company, Corporate Engineering Division
Shiga, Japan
Tel: +81-77-562-5658, fax: +81-77-563-1967

* Corresponding Author

ABSTRACT

With the aim of developing a method for reducing energy consumption of room air conditioners, we address a higher-efficiency design of the rotary compressor currently most used worldwide. We focused on a new rotary compressor equipped with a mechanism to restrict the rolling motion of the piston, and performed a dynamics analysis. The new rotary compressor has a small pillar at the tip of the vane and constitutes a turning-pair of the vane and the piston, which limits the rolling motion of the piston. By limiting piston rotation, heat transfer to the suction process from the compression chamber will be suppressed, and we can expect higher compression efficiency. Before investigating the compression efficiency, we performed a dynamics analysis of this new rotary compressor and examined the forces and dynamic behavior of its components, as well as the mechanical efficiency of the compressor. We realized the following results: First, we clarified the contact point between the vane tip and the piston in the turning-pair by considering the equilibrium of forces and moments acting on the vane; second, by reducing the vane tip radius, the friction loss related to the vane is reduced, and the mechanical efficiency is improved; and third, the new rotary compressor has less vane tip friction loss and, on the other hand, slightly higher friction loss between the vane side and the cylinder compared with the rolling-piston rotary compressor. Consequently, the new rotary compressor would have a slightly higher mechanical efficiency.

1. INTRODUCTION

In recent years, with the aim of controlling global warming, there has been a strong demand from society to reduce energy consumption of home appliances. In Japan, room air conditioners occupy a quarter of the electric power usage in households, and the compressor constitutes 80% of power consumption of room air conditioners. Therefore, saving energy by improving compressor efficiency is a significant issue.

The rolling-piston rotary compressor is used mainly in the room air conditioners, and many studies for its high-performance have been carried out. Ishii *et al*. (1990) performed a dynamics analysis of the rolling-piston rotary compressor, and showed optimum combinations for high mechanical efficiency. Ishii *et al*. (2010) also showed net efficiency simulation method of the rolling-piston rotary compressor for its optimal performance. Also Ito *et al*. (2010) studied the rolling motion of the piston. This rotary compressor is characterized by the rolling motion of the piston; the rolling piston transfers the heat to low-temperature refrigerant in the suction process from high-temperature refrigerant after compression, resulting in refrigerant heating loss.

Recently, Kario *et al*. (2010) suggested a new rotary compressor (as it is hereinafter called) equipped with a mechanism to restrict the rolling motion of the piston, engaging the vane and the piston with a turning-pair. Restricting the rolling motion controls the heat transfer by the piston, and reduces heating loss of the suction refrigerant; therefore, higher compression efficiency can be expected. Total compressor efficiency is calculated as the product of the mechanical efficiency and the compression efficiency; therefore, in developing the new compressor, both efficiencies should be investigated. In this study, we performed a dynamics analysis of the new rotary compressor, and then investigated the forces acting on each part and the relationship between vane and piston as well as the mechanical efficiency. We also performed a dynamics analysis of the rolling-piston rotary compressor with the same conditions as the new rotary compressor, and compared the dynamics properties of both compressors. In addition, this comparison of dynamics properties was performed with "one-piston rotary," which has a paired piston and cylinder.

2. THEORETICAL ANALYSIS

2.1 New Rotary-Compression Mechanism and Its Operation

The new rotary compressor has almost the same elements as the rolling-piston rotary compressor; however, it has a small pillar at the tip of the vane, which constitutes a turning-pair of vane and piston, limiting the rolling motion of the piston. Figure 1 shows the compression process of the new rotary compressor.

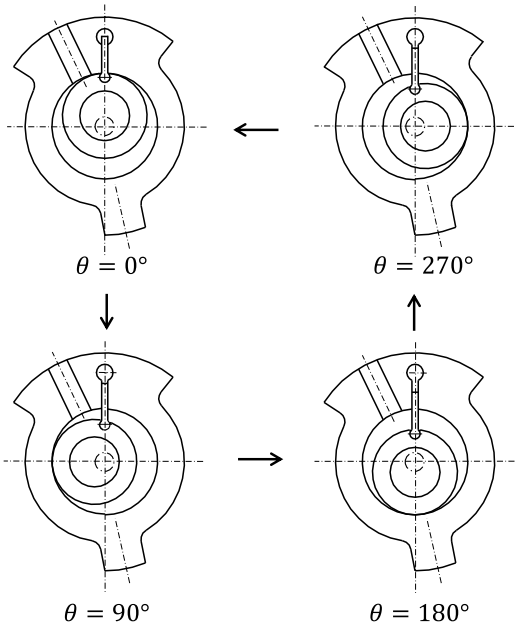

Figure 1: Compression process of new rotary compressor

2.2 Coordinate System and Dynamics Model

The coordinate system and main variables used to perform the dynamics analysis of the new rotary compressor are shown in Figure 2. We placed the origin of the x-y coordinate system in the cylinder center and defined x-axis in the vane moving direction. We defined the rotating angle of the crankshaft as θ and the counterclockwise direction of crank angle θ as positive. Also, we defined the oscillating angle of the piston as ξ, which is formed between the x-axis and the line connecting the piston center O_p and pillar center O_v of the vane tip.

As shown in Figure 3, we defined the contact angle of the vane tip and the piston as ψ, which is formed between the x-axis and the line connecting the pillar center O_v and the contact point of the vane tip and the piston. We assumed that the suction pressure P_s was applied to the vane tip clearance of the suction side of the contact point ψ, and compression-chamber pressure P_c was applied to the vane tip clearance of the compression-chamber side of the contact point ψ. We treated the contact angle ψ as an unknown variable, which would be determined by balancing the forces and moments that act on the vane.

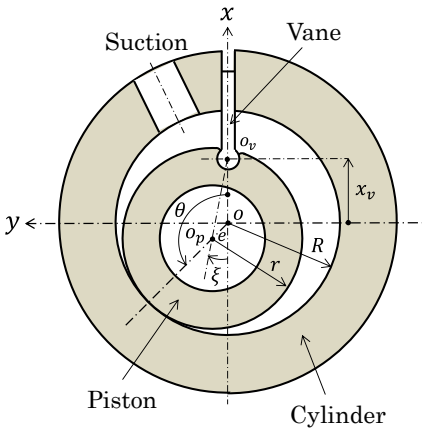

Figure 2: Coordinate system and main variables

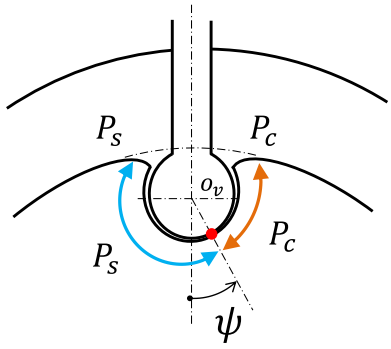

Figure 3: Contact point between vane tip and piston, and pressure distribution around vane tip

2.3 Equations of Motion for Vane

Figure 4 shows the analytical model of the vane. We obtained Equations (1)–(3) of motion of the vane based on this model.

Equation of motion in the *x*-axis direction:

$$m_v\ddot{x}_v = F_{qx} + F_{gt1} + F_{gt2} + F_v + F_{hf} + F_d + F_{vp}\,sin\xi \tag{1}$$

Equation of motion in the *y*-axis direction:

$$F_{qy} - F_{vf} + F_h + F_{gn1} - F_{gn2} + F_{vp}\,cos\xi = 0 \tag{2}$$

Equation of motion relating to rotation:

$$(R + b - x_v)F_{gn1} + aF_{gt1} - (R - x_v)F_{gn2} - aF_{gt2} + M_q - r_vF_{vp} + r_v\sqrt{{F_{vf}}^2 + {F_{hf}}^2} = 0 \tag{3}$$

In formulating equations of motion for the vane, the contact force F_{vn} and friction force F_{vt} between the vane tip and piston were decomposed into horizontal and vertical components as shown in Figures 5 and 6, respectively. These relations are expressed as Equations (4) and (5), respectively. By this method, unknown variable ψ does not appear as the form of the trigonometric function in Equations (1)–(3). As a result, we were able to obtain the convergence solution of ψ through numerical calculation.

$$F_v = F_{vn}cos\psi\ ,\ F_h = F_{vn}sin\psi \tag{4}$$

$$F_{vf} = F_{vn}cos\psi\ ,\ F_{hf} = F_{vn}sin\psi \tag{5}$$

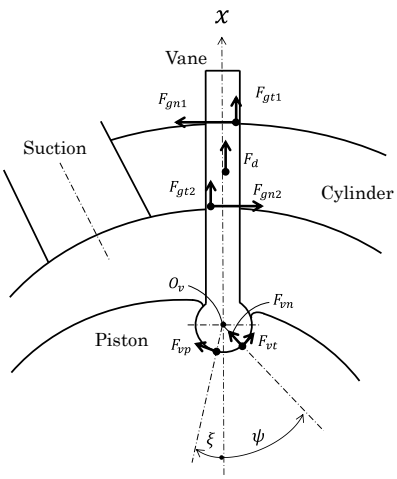

Figure 4: Analytical model of vane

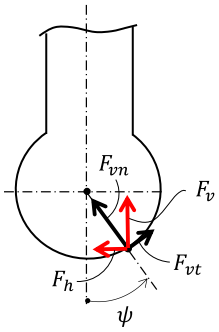

Figure 5: Contact force F_{vn} between vane tip and piston

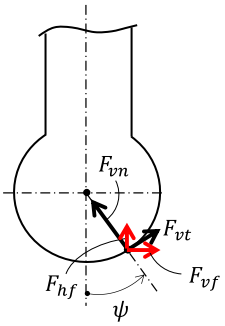

Figure 6: Friction force F_{vt} between vane tip and piston

2.4 Equations of Motion for Piston

Figure 7 shows the analytical model of the piston. We obtained Equations (6)–(8) of motion of the piston based on this model.

Equation of motion in the *x*-axis direction:

$$m_p\ddot{x}_{op} = F_{en}cos\eta - F_v - F_{hf} - F_{cn}cos\theta + F_{ct}sin\theta + F_p sin(\beta + \gamma) + F_a sin\theta - F_{vp}sin\xi \quad (6)$$

Equation of motion in the *y*-axis direction:

$$m_p\ddot{y}_{op} = F_{en}sin\eta - F_h + F_{vf} - F_{cn}sin\theta - F_{ct}cos\theta + F_p cos(\beta + \gamma) - F_a cos\theta - F_{vp}cos\xi \quad (7)$$

Equation of motion relating to rotation:

$$I_p\ddot{\xi} = (r - h_p)\, sin(\xi + \psi)\, F_{vn} - \{(r - h_p)\, cos(\xi + \psi) - r_v\}F_{vt} + (r - h_p - r_v)F_{vp} + l_f F_p + rF_{ct} - M_p - M_a \quad (8)$$

2.5 Equation of Motion for Crankshaft

Figure 8 shows the analytical model of the crankshaft. We obtained Equations (9)–(11) of motion of the crankshaft based on this model.

Equation of motion in the *x*-axis direction:

$$m_c\ddot{x}_{oc} = F_{gx} - F_{en}cos\eta \quad (9)$$

Equation of motion in the *y*-axis direction:

$$m_c\ddot{y}_{oc} = F_{gy} - F_{en}sin\eta \quad (10)$$

Equation of motion relating to rotation:

$$I_c\ddot{\theta} = M_m - eF_{en}sin(\eta - \theta) - M_p - M_s \quad (11)$$

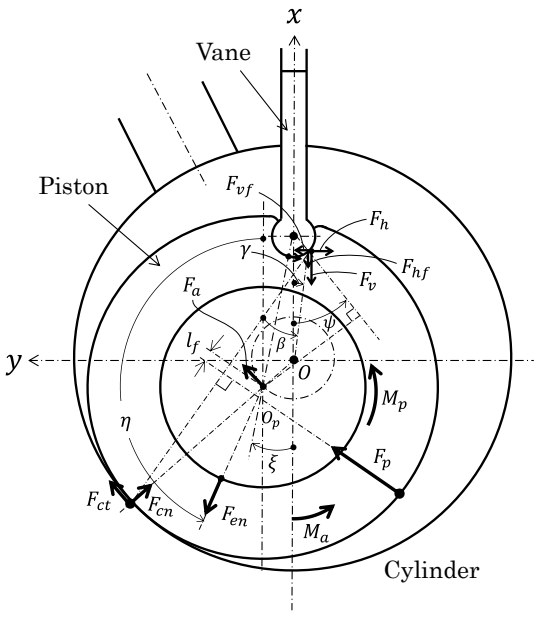

Figure 7: Analytical model of piston

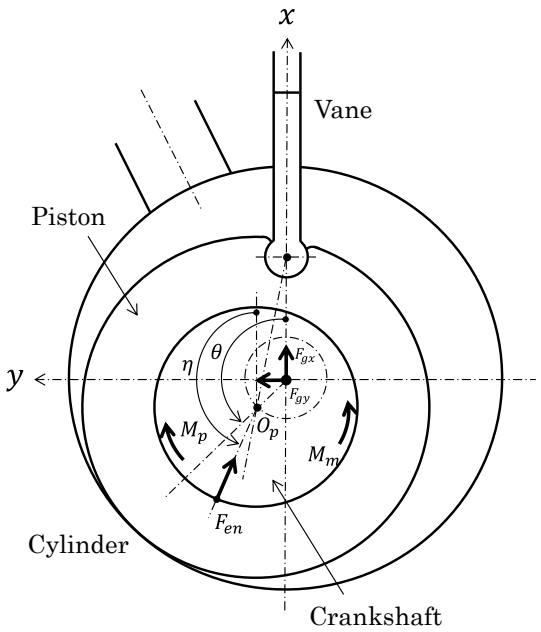

Figure 8: Analytical model of crankshaft

2.6 Transformation of Equation for Crankshaft

We obtained the transformed Equation (12) for the crankshaft from Equation (11), eliminating the force F_{en} and the angle η by using Equations (6) and (7).

$$\left(I_c + m_p e^2\right)\ddot{\theta} = M_m + e\frac{sin(\theta-\psi)}{cos\psi}m_v\ddot{x}_v + e\frac{cos\theta}{cos\psi}F_{vt} - e\,cos\alpha\cdot F_p - e\frac{sin(\theta-\psi)}{cos\psi}F_{qx}$$
$$-e\frac{sin(\theta-\psi)}{cos\psi}\left(F_{gt1} + F_{gt2} + F_d\right) - e\frac{cos\theta\,cos(\xi+\psi)}{cos\psi}F_{vp} - eF_{ct} - eF_a - M_p - M_s \quad (12)$$

The left-hand side of Equation (12) represents the angular acceleration of the crankshaft and the right-hand side represents each torque affecting angular acceleration. The first term of the right-hand side of Equation (12) is expressed as motor torque, the second term as inertia torque of the vane, the third term as friction torque of the vane tip, the fourth and fifth terms as gas compression torque, the sixth term as friction torque of the vane side, the seventh term as viscosity friction torque of the vane tip, the eighth, ninth, and tenth terms as friction torque relating to the piston, and the eleventh term as friction torque between the crankshaft and bearings.

By solving Equation (12) through numerical calculation, we can identify the rotating behavior of the crankshaft and the forces acting on each part. Moreover, we can obtain the mechanical loss at each sliding part by numerical integration of each term of the right-hand side of Equation (12).

3. NUMERICAL ANALYSIS

3.1 Process of Numerical Analysis

We performed the numerical analysis as follows:

(a) Set the initial parameters.
(b) Simultaneously solved four linear equations, (1), (2), (3), and (8), to obtain the vane contact angle ψ and forces $(F_{gn1}, F_{gn2}, F_{vn})$ acting on the vane on each crank angle $\theta(i)$.
(c) Found the angular velocity $\dot{\theta}(i+1)$ and crank angle $\theta(i+1)$ using the Runge-Kutta method.
(d) Repeated Steps (b) and (c) around one revolution of the crankshaft.
(e) Evaluated whether the initial value of $\dot{\theta}$ coincided with its final value.
(f) Terminated the analysis when both values coincided, calculating the sliding loss in each part and the mechanical efficiency of the compressor.

3.2 Specifications of Numerical Analysis

3.2.1 Compressor specifications

Table 1: Compressor specifications (with a paired piston and cylinder)

Vane thickness	$2a$	mm	3.2
Eccentricity	e	mm	4.0
Cylinder depth, piston length	l_{cy}	mm	14.0
Cylinder radius	R	mm	21.5
Piston inner radius	r_c	mm	11.0
Piston outer radius	r	mm	17.5
Crankshaft radius	r_s	mm	8.0
Suction volume	V_s	cm^3/rev	13.5
Mass of crankshaft and motor	m_c	kg	1.4
Inertia moment of crankshaft and motor	I_c	$kg\cdot mm^2$	520

3.2.2 Sliding loss and friction coefficient

The new rotary compressor has three main sliding locations, as shown in Table 2. It is assumed that each sliding location is in mixed lubrication. Considering that, we calculated the sliding loss of the each location with friction coefficients as shown in Table 2. Also, these friction coefficients were used in the analysis of the rolling-piston rotary compressor.

Table 2: Friction coefficients

Sliding location	Friction coefficient μ
(1) Vane/cylinder	0.083
(2) Vane/piston	0.083
(3) Crankshaft/bearing	0.013

3.2.3 Analysis conditions

Table 3: Operating conditions at the numerical analysis

	Crankshaft rotating speed [rps]	Suction pressure [MPa]	Discharge pressure [MPa]
(1) Rated condition	57.5	1.0	3.4
(2) Low-speed condition	20.0	1.3	2.5

Refrigerant: R410A

3.2.4 Analysis parameter of new rotary compressor

We investigated the mechanical characteristics of the new rotary compressor with changing the vane tip radius $r_v = 1.5 - 3.0\ mm$.

4. CALCULATION RESULTS AND DISCUSSION

4.1 Calculation Results of New Rotary Compressor

Figure 9 shows the compression-chamber pressure P_c on the crank angle θ. Figures 10 and 11 show the angular acceleration $\ddot{\theta}$ and the angular velocity $\dot{\theta}$ of the crankshaft, respectively. From Figures 9, 10, and 11, it can be seen that the compression torque increases when the pressure P_c increases, the angular acceleration $\ddot{\theta}$ becomes negative, and the angular velocity $\dot{\theta}$ decreases. Also, it is possible to identify the rotational behavior of the crankshaft from Figure 11. With the specifications of this new rotary compressor, the velocity fluctuation rate of the crankshaft is approximately 14% at Rated Condition and the velocity fluctuation rate increases to 55% at Low-speed condition. These rotational behaviors of the crankshaft were the same in the case of the rolling-piston rotary compressor.
Here, the velocity fluctuation rate of the crankshaft is defined as the following equation:

$$\text{Velocity fluctuation rate} = \frac{\text{fluctuation of angular velocity}}{\text{average of angular velocity}} \times 100 \quad [\%]$$

Figures 12 and 13 show the contact forces F_{gn1}, F_{gn2} between the vane and the cylinder at Rated condition. Both contact forces are small between $0° \le \theta \le 180°$ of crank angle θ in which pressure P_c is relatively low; however, when the pressure P_c increases in the crank angle θ more than 180°, both contact forces increase rapidly, because the vane is pushed to the cylinder wall in the vane slot. Also, even if vane tip radius r_v changes, the contact forces F_{gn1}, F_{gn2} remain unchanged. Figure 14 shows the comparison of the contact force F_{gn2} on the new rotary compressor and the rolling-piston rotary compressor. It is feared that friction loss between the vane and the cylinder increases slightly because the absolute value of the contact force F_{gn2} on the new rotary compressor is slightly larger than on the rolling-piston rotary compressor.

Figure 15 shows the changes of the contact point ψ of the vane tip with the crank angle θ at Rated condition. This figure shows that the contact point ψ moves to the suction side when the crank angle θ advances and the pressure P_c increases. Moreover, it moves to the suction side when the vane tip radius r_v increases. On the new rotary compressor, a rotational moment to the clockwise direction by refrigerant-gas force F_p acts on the piston. Therefore, when vane tip radius r_v or refrigerant-gas force F_p increases, this rotational moment increases and the contact point ψ moves to the suction side, as shown in Figure 15.

Figure 16 shows the contact force F_{vn} between the vane tip and the piston. This contact force F_{vn} decreases as the contact point ψ moves to the suction side. This is because the high-pressure gas has entered into the clearance between vane tip and piston from the compression chamber to reduce the contact force when the contact point moves to the suction side. Figure 17 shows a comparison of the vane tip contact force F_{vn} for the new rotary compressor and the rolling-piston rotary compressor. The contact force F_{vn} of the new rotary compressor significantly decreased compared to the rolling-piston rotary compressor in the crank angle θ more than 180°, therefore it is expected that the friction loss between vane and piston decreases.

Figure 18 shows the relationship between mechanical efficiency η_m and vane tip radius r_v in Rated condition. It indicates that the mechanical efficiency of the new rotary compressor would be improved when the vane tip radius r_v decreases. This is because two friction losses related to the vane decrease when the vane tip radius r_v becomes small, as shown in Figure 19. From these calculation results, it is desirable for the vane tip radius to be smaller as far as possible in mass production.

4.2 Mechanical Efficiency of New Rotary Compressor and Rolling-Piston Rotary Compressor

Table 4 shows calculation results of the loss (power) analysis and mechanical efficiency of the new rotary and rolling-piston rotary compressor. At Rated condition, the friction loss between the vane and the piston in the new rotary compressor decreases because the contact force F_{vn} of the vane tip decreases. On the other hand, the friction loss between the vane and the cylinder increases because the contact forces F_{gn1}, F_{gn2} slightly increase. After these changes in friction loss, mechanical efficiency of the new rotary compressor is slightly higher than that of the rolling-piston rotary compressor. On the other hand, the calculation results at Low-speed condition show that the loss (power) in both compressors is almost the same, so both compressors have almost the same mechanical efficiency. Consequently, it became clear that the new rotary compressor would have a higher mechanical efficiency than the rolling-piston rotary compressor.

5. CONCLUSION

We performed the dynamics analysis of the new rotary compressor equipped with a mechanism to restrict the rolling motion of the piston, engaging the vane and the piston with a turning-pair. We investigated the forces acting on each part, behavior of vane and piston, and mechanical efficiency, and we obtained the following conclusions.

(1) The mechanical efficiency of the new rotary compressor would improve as the vane tip radius decreases.
(2) In the new rotary compressor, the contact force of the vane tip becomes small and the friction loss decreases between the vane and the piston. Meanwhile, the friction loss between the vane and the cylinder increases slightly. After these changes in friction loss, the mechanical efficiency of the new rotary compressor would be slightly higher than that of the rolling-piston rotary compressor.

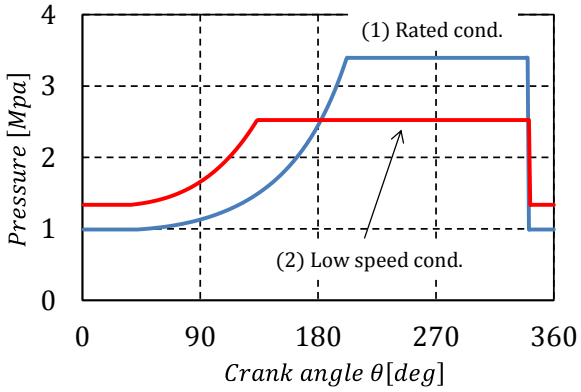

Figure 9: Pressure P_c of compression-chamber

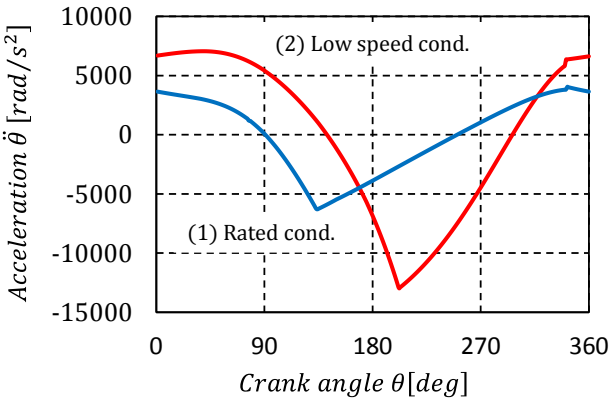

Figure 10: Angular acceleration of crankshaft

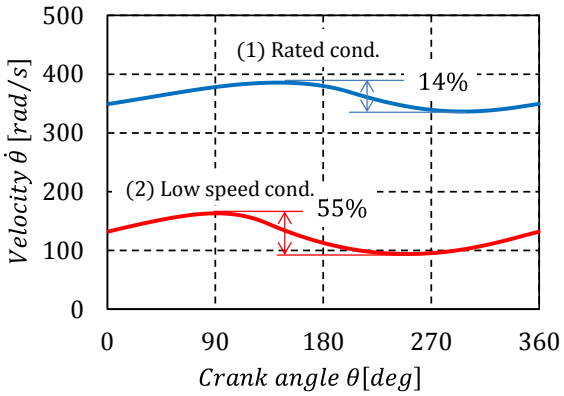

Figure 11: Angular velocity of crankshaft

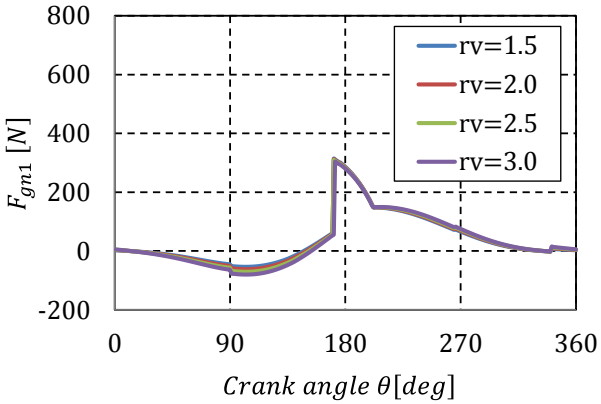

Figure 12: Contact forceF_{gn1} between vane and cylinder

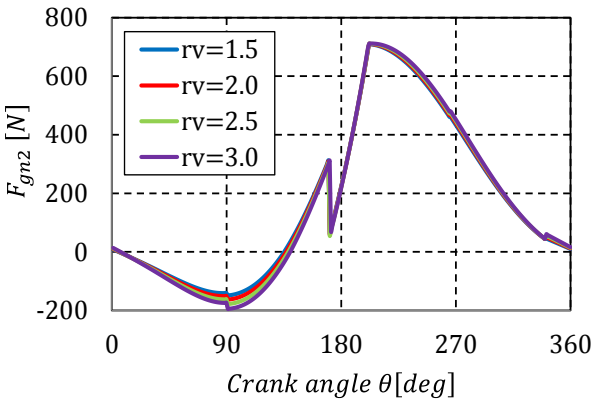

Figure 13: Contact forceF_{gn2} between vane and cylinder

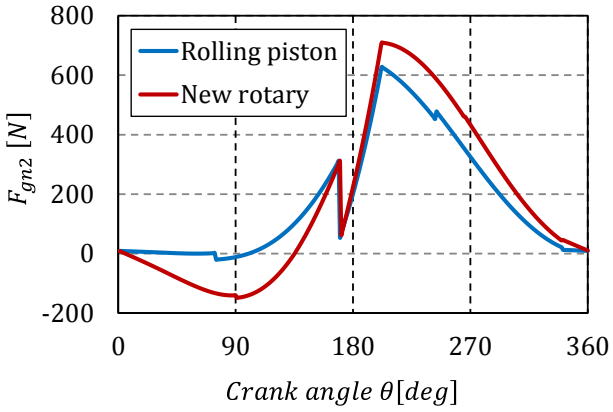

Figure 14: Comparison of contact force F_{gn2}

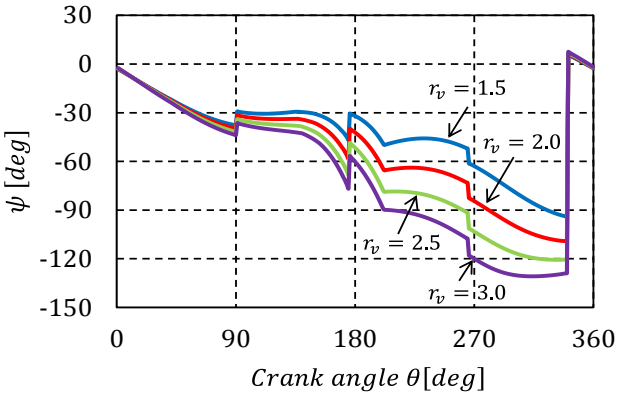

Figure 15: Contact angle ψ of vane tip and piston

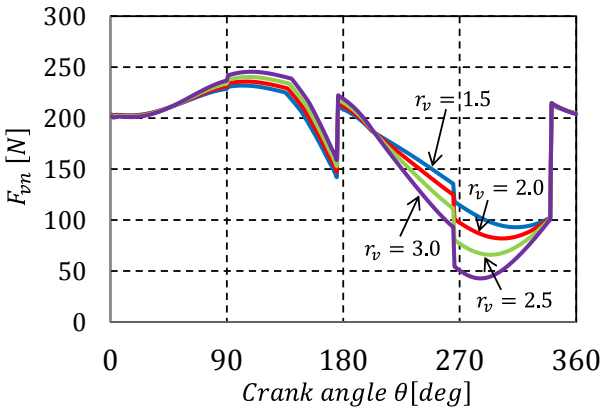

Figure 16: Contact force F_{vn} between vane tip and piston

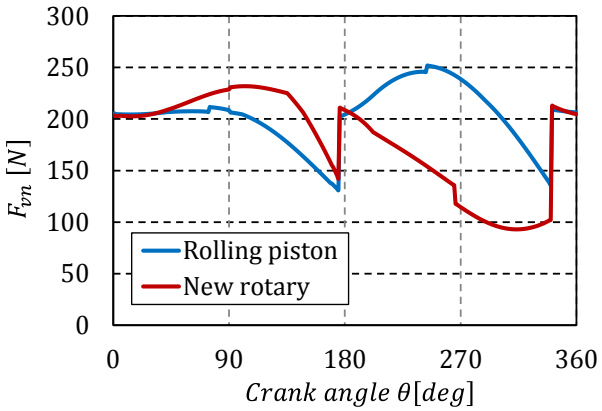

Figure 17: Comparison of contact force F_{vn} (New rotary vs. Rolling-piston rotary)

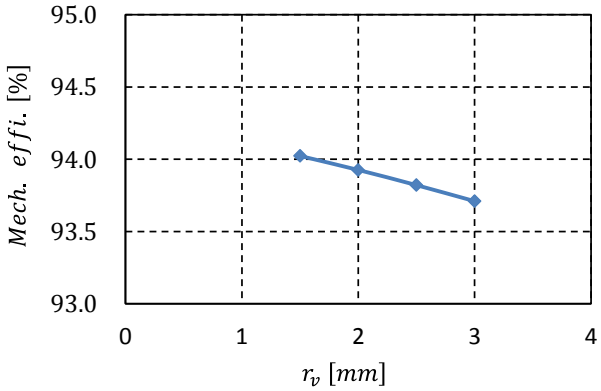

Figure18: Relationship between vane tip radius and mechanical efficiency

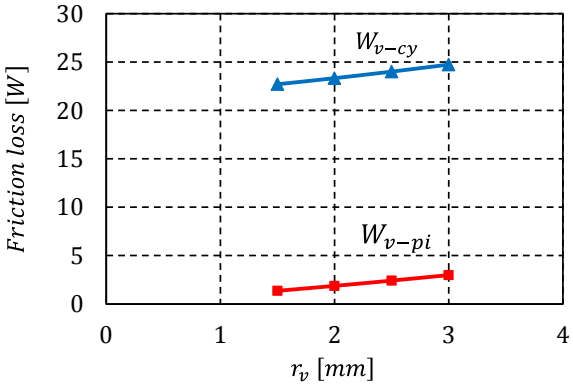

Figure19: Relationship between vane tip radius and mechanical loss on vane

Table4: Comparison of losses and mechanical efficiency between new rotary compressor and rolling-piston rotary compresso Unit [W]

Mechanical loss (Power)	(1) Rated condition		(2) Low-speed condition	
	New rotary	Rolling piston	New rotary	Rolling piston
Theoretical compression power	1029.7	1029.0	239.6	239.4
Crankshaft bearing loss	36.8	36.7	7.9	7.8
Friction loss at vane/piston	1.4	11.2	0.2	0.1
Friction loss at vane/cylinder	22.7	16.0	3.5	3.3
Friction loss at piston/crank-pin	3.9	4.0	0.5	0.5
Friction loss at piston/cylinder	2.0×10^{-4}	2.0×10^{-4}	2.0×10^{-5}	2.0×10^{-5}
Friction loss at piston end face	0.65	0.65	0.08	0.08
Friction loss at vane end face	0.05	0.05	0.006	0.007
Total power	1095.0	1097.7	251.7	251.3
Mechanical efficiency $= \frac{\text{Theoretical compression power}}{\text{Total power}}$	0.940	0.937	0.952	0.952

NOMENCLATURE

e	eccentricity	(mm)
F_a, F_d	friction force on piston end face, on vane end face	(N)
F_{cn}	lifting force acting on piston by refrigerant	(N)
F_{ct}	friction force by refrigerant between piston and cylinder	(N)
F_{en}	oil film force between piston and crank-pin	(N)
F_{gn1}, F_{gn2}	contact forces between vane and cylinder	(N)
F_{gt1}, F_{gt2}	friction force caused by F_{gn1}, F_{gtn2}	(N)
F_p	refrigerant-gas force acting on piston	(N)
F_{qx}, F_{qy}	refrigerant-gas forces acting on vane	(N)
F_{vn}	contact force between vane tip and piston	(N)
F_{vp}	friction force by oil film around vane tip	(N)
F_{vt}	friction force caused by F_{vn}	(N)
h_p	length between piston surface and pillar center of vane tip	(mm)
$I_c,\ I_p$	inertia moment of crankshaft and motor, of piston	$(kg\ mm^2)$
l_{cy}	cylinder depth, piston length	(mm)
l_f	distance between F_p acting line and piston center O_p	(mm)
$m_c,\ m_p,\ m_v$	mass of crankshaft and motor, of piston, of vane	(kg)
M_a	friction moment acting on piston end face	(Nmm)
M_m	motor torque	(Nmm)
M_p	friction moment by oil film between crank-pin and piston	(Nmm)
M_s	friction moment between crankshaft and bearing	(Nmm)
P_c	pressure of compression-chamber	(MP_a)
$P_d,\ P_s$	discharge pressure, suction pressure	(MP_a)
$R,\ r,\ r_c$	cylinder radius, piston outer radius, piston inner radius	(mm)
$r_s\ ,\ r_v$	crankshaft radius, pillar radius of vane tip	(mm)
x_v	position of the vane tip in the x-direction	(mm)
β, γ	angles of contact points between vane and piston and cylinder	(rad)
η	angle between force F_{en} and x-axis	(rad)
θ	rotating angle of crankshaft	$(rad\ or\ ^\circ)$
μ	friction coefficient	(-----)
$\xi\ , \psi$	oscillating angle of piston, angle of vane tip contact point	$(rad\ or\ ^\circ)$

REFERENCES

Ishii, N., Fukushima, M., Yamamura, M., Fujiwara, S., Kakita, S., 1990, Optimum Combination of Dimensions for High Mechanical Efficiency of a Rolling–Piston Rotary Compressor, Proc. of Int. Comp. Eng. Conf. at Purdue, Vol. 1, pp. 418-424.

Ishii, N., Morita, N., Ono, M., Yamamoto, S., Sano, K., 2000, Net Efficiency Simulations of Compact Rotary Compressors for Its Optimal Performance, Proc. of Int. Comp. Eng. Conf. at Purdue, Vol. I, pp. 475-482.

Ito, Y., Hattori, H., Miura, K., 2010, Numerical Analysis for Rotating Motion of a Rolling Piston in Rotary Compressors, - Effective Factors for Characteristics of Rotating Motion of a Rolling Piston -, Proc. of 20th Int. Comp. Eng. Conf. at Purdue,1217

Karino, T., Hiwata, A., Nakano, M., Funakoshi, D., Sawai, K., Iida, N., Fukuhara, H., Murakami, H., Tsujimoto, T.,2010, ROTARY COMPRESSOR, PCT (Patent-Cooperation-Treaty),WO2010/073426